

## Synthesis and Characterization of Brush-Like ZnO Nanorods using Albumen as Biotemplate

Fatemeh Nouroozi and Faezeh Farzaneh\*

Department of Chemistry, University of Alzahra, Vanak, Tehran, Iran

Nanobastões de ZnO com morfologia similar à de escovas, estrutura cristalina do tipo wurtzita (hexagonal), diâmetro médio de 90 nm e comprimento  $\geq 1 \mu\text{m}$ , foram preparados por calcinação (700 °C) do material híbrido (Zn(II)/albumina) obtido pelo método sol-gel reagindo-se acetato de zinco e clara de ovo, em meio aquoso. O material foi caracterizado por difratometria de raio-X de pó (XRD), microscopia eletrônica de varredura (MEV) e de transmissão (TEM), análise termogravimétrica (TGA/DTA), e espectroscopia FT-IR e de fotoluminescência (PL). A área superficial foi determinada como sendo igual a  $6,91 \text{ m}^2 \text{ g}^{-1}$  pelo método BET. Os eventos térmicos no TGA/DTA foram consistentes com a decomposição da albumina a 300 °C e a formação final de ZnO em 578,5 °C. Os resultados mostraram que a albumina desempenha papel essencial na formação dos nanobastões de ZnO, atuando como molde.

Crystalline ZnO nanorods with wurtzite-like structure and average diameter of 90 nm and length  $\geq 1 \mu\text{m}$ , was prepared by calcination (700 °C) of a Zn(II)/albumen hybrid obtained by sol-gel method, by the reaction of Zn(II) acetate and egg white (albumen), in aqueous solution. The material was characterized by powder X-ray diffraction (XRD), scanning electron (SEM) and transmission electron microscopy (TEM), thermogravimetric analysis (TGA/DTA),  $\text{N}_2$  adsorption/desorption (BET method), FT-IR and photoluminescence (PL) spectroscopy. The surface area was determined to be  $6.91 \text{ m}^2 \text{ g}^{-1}$  by BET method. The TGA/DTA thermal events were consistent with the decomposition of albumen at 300 °C and final formation of ZnO at 578.5 °C. The results showed that albumen act as template playing essential role on defining the formation of ZnO nanorods with brush-like morphology.

**Keywords:** brush-like ZnO nanorods, sol-gel method, egg white (albumen)

### Introduction

In recent years, there have been many reports on novel preparation and characterization methods of nanomaterials, based on metal oxide semiconductors in general and ZnO in particular, owing to their special properties.<sup>1</sup> ZnO nanoparticles, with a wide band gap has found to be an efficient candidate for utilization in optical devices operating at room temperature, because of their catalytic/photocatalytic activity and use as CO gas sensor. Furthermore, ZnO is a material with excellent chemical, thermochemical and mechanical stability, which can be used to absorb ultraviolet light, protecting us against this hazardous radiation.<sup>2</sup>

Nanostructured ZnO with as different shapes as one dimensional (1D) nanowires,<sup>3-7</sup> nanotubes,<sup>8,9</sup>

nanorods<sup>10</sup> and nanobelts,<sup>11</sup> two dimensional (2D) nanostructures such as nanosheets<sup>12</sup> and nanowalls<sup>13</sup> and some three dimensional (3D) nano/microstructures such as nanoflower and tetrapod like structures,<sup>14-17</sup> have been fabricated by means of various methods. Thus, the fabrication methods of ZnO nanomaterials can be classified into two categories: (i) vapor phase processes and (ii) solution phase routes.<sup>18-23</sup> Recently, solution phase routes including microemulsion,<sup>23</sup> solvothermal,<sup>14</sup> hydrothermal,<sup>24</sup> self-assembly and template assisted sol-gel methods have been utilized for the synthesis of ZnO nanostructures.<sup>22,25-27</sup> However, to the best of our knowledge, few are the reports on the utilization of biotemplates for the synthesis of ZnO nanostructures.<sup>28</sup> Here we disclosure a new method for the preparation of brush-like ZnO nanorods using albumen as a natural and nontoxic template, and water as a green solvent.

\*e-mail: faezeh\_farzaneh@yahoo.com, farzaneh@alzahra.ac.ir

## Experimental

### Equipments and methods

The characterization by XRD was carried out in a Siefert 3003PTS diffractometer, using  $\text{CuK}\alpha$  ( $\lambda = 1.5406 \text{ \AA}$ ) radiation and 0.4 g of the powder material, enough to the cavity of the sample holder. The samples for scanning electron microscopy (Phillips XL30) were prepared by depositing the material on brass holders and coating them with a thin layer of gold. Transmission electron microscopy images were recorded using a Philips CM200 microscope equipped with a Field Emission Gun. The samples were prepared by dispersing the powdered material in methanol and transferring a drop to copper grids (Cu-200 mesh) coated with a thin layer of carbon, and letting dry at room temperature. This process was repeated 3 or 4 times to assure an enough amount of material deposited on the grid. Infrared spectra were registered in a Bruker, Tensor 27 DTGS FT-IR equipment in the 400 to 4000  $\text{cm}^{-1}$  range, using samples prepared in KBr pellets (5 mg *per* 100 mg KBr). Photoluminescence spectra were recorded in a Perkin Elmer LS-55 spectrofluorometer equipped with pulse Xenon lamp, using a triangular quartz cell. Thermoanalytic measurements (PLSTA 1500 TGA/DTA) were carried out in air (flow = 75  $\text{mL min}^{-1}$ ), in the 25 to 900  $^{\circ}\text{C}$  range, and temperature gradient of 10  $\text{K min}^{-1}$ . The  $\text{N}_2$  adsorption/desorption measurements (Belsorp mini-II instrument) were carried out at 77 K. Samples were heated at 473 K at a rate of 4  $\text{K min}^{-1}$ , followed by degassing at this temperature for 2 h under vacuum ( $1 \times 10^{-5}$  mbar), and  $\text{N}_2$  was introduced by pulse method for several times.

### Synthesis of ZnO using albumen as biotemplate

All reagents were of analytical grade and purchased from Merck Chemical Company. In a typical procedure, egg white (albumen, 15 g) was slowly added into a magnetically stirred solution of Zn(II) acetate (25 mmol) in distilled water (20 mL), at room temperature. After vigorous stirring for 10 min, the white solid was filtered and carefully washed with distilled water. Then, distinct samples were calcined at 400, 500, 600 and 700  $^{\circ}\text{C}$ , for 3 h, and characterized.

## Results and Discussion

### XRD characterization

The XRD patterns of ZnO before and after calcination at increasingly higher temperatures are shown in Figure 1. As can be inferred from the noisy and structureless diffractogram

shown in Figure 1a, the white precipitate obtained by the reaction of Zn(II) salt and albumen is amorphous, probably due to the presence of the organic phase. However, low intensity and narrow peaks was observed after calcination at 400  $^{\circ}\text{C}$ , indicating the onset temperature for formation of a crystalline phase. The amount of crystalline phase increased as a function of temperature (Figure 1b-1e), such that intense and sharp peaks were observed for the material calcined at 700  $^{\circ}\text{C}$ , as expected for a highly crystalline material. The peaks located at diffraction angles ( $2\theta$ ) of 31.18, 33.87, 35.68, 47.00, 56.16, 62.42, 67.47 and 68.46 (Figure 1e) can be assigned to the reflections from 100, 002, 101, 102, 110, 103, 112 and 201 crystal planes, respectively, of a material with wurtzite-like structure. In fact, those data are consistent with those published in JCPD standard card No. 36-1451 (Zincite, hexagonal, P63mc space group, unit cell parameters:  $a = 0.324 \text{ nm}$ ,  $c = 0.5192 \text{ nm}$  and  $Z = 2$ ).<sup>29</sup>

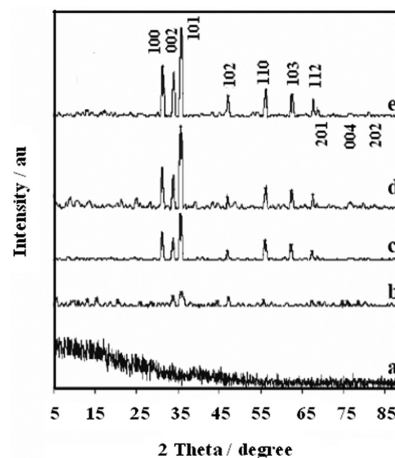


**Figure 1.** XRD patterns of (a) as-prepared Zn(II)/albumen hybrid, and after heat treatment at (b) 400, (c) 500, (d) 600, and (e) 700  $^{\circ}\text{C}$ , in one atmosphere, for 3 h.

Surface area of the ZnO/albumin calcined at 700  $^{\circ}\text{C}$ , was determined to be 6.91  $\text{m}^2 \text{g}^{-1}$ , by BET method. For example, recently Bhattacharyya and Gdanken<sup>30</sup> have reported the synthesis of ZnO nanodisks with particle size and surface area of 400 nm and 3  $\text{m}^2 \text{g}^{-1}$ , respectively.<sup>30</sup> This is a clear indication that the surface area depends on average particle size and morphology of nanoparticles.

### SEM and TEM studies

Scanning and transmission electron microscopy studies were carried out in order to confirm the morphology, size and structure of the crystallites. Typical SEM images of ZnO/albumen hybrid, calcined at 700  $^{\circ}\text{C}$  for 3 h, are shown in Figures 2a-d. As can be seen, a large amount of nanorods with more or less homogeneous diameter (*ca.* 90 nm)

and length (*ca.* 1.1  $\mu\text{m}$ ) was revealed. Interestingly, they seem to grow on the top of a thin layer of densely packed, much shorter nanorods and nanoparticles, giving rise to a brush-like morphology (Figures 2c-d). In fact, more detailed characterization by TEM revealed the formation of nanorods with hexagonal crystal structure, as shown in Figure 3. The diffraction pattern of a selected area (SEAD) is shown in the inset, confirming their high crystallinity, and that are growing along the 001 plane. To the best of our knowledge, this is the first time that such a simple method was used to prepare ZnO nanorods, revealing the significance of our contribution to materials science field. The size distribution histograms based on diameter and length are shown in Figures 2e and 2f, respectively.

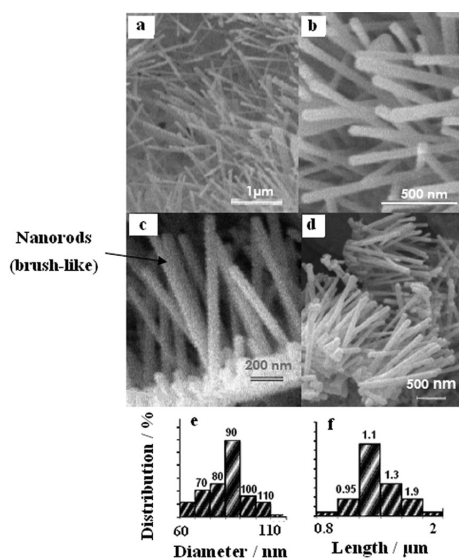


**Figure 2.** SEM images of ZnO nanorods calcined at 700 °C for 3 h, (a, b) at two different magnifications, and showing the (c, d) brush-like morphology. The size distribution histograms for diameter and length (e, f), respectively, are also shown.

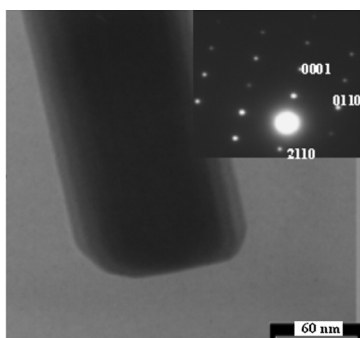


**Figure 3.** TEM image of a typical ZnO nanorod, and respective diffraction pattern (SAED) of a selected area (inset).

#### TGA study

In order to improve the understanding on the preparation method, the thermal behavior (up to 900 °C) was

investigated by TGA/DTA. A typical profile of the as-prepared Zn(II)/albumen hybrid is shown in Figure 4. The thermal decomposition takes place in three steps. The first endothermic process, with weight loss of 8%, is observed up to 100 °C and can be assigned to the loss of weakly bond water molecules. The second exothermic event occurred in a much broad temperature range (200 to 500 °C), encompassing a weight loss of 50%, is consistent with the decomposition of the albumen template. The third process at 578.5 °C perhaps due to the organic residue decomposition (34%), leading to the formation of zinc oxide with wurtzite-like structure, which is stable up to 900 °C. This reaction is consistent with the sharp exothermic peak observed in the corresponding DTA curve.

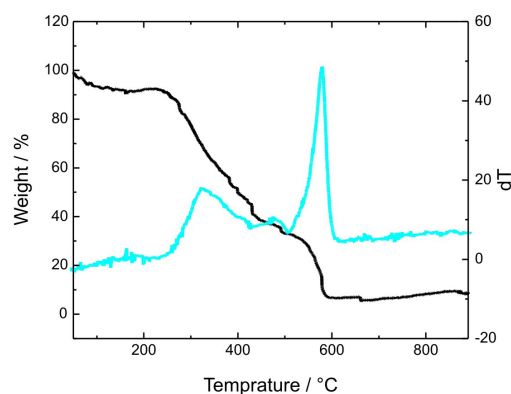


**Figure 4.** TGA and DTA curves of as-prepared Zn(II)/albumen hybrid.

#### FTIR study

The FTIR spectra of pure albumen and as-prepared Zn(II)/albumen hybrid are shown in Figures 5a and 5b, respectively. They are very similar exhibiting characteristic peaks at 3275, 3042, 2922, 1655 and 1526  $\text{cm}^{-1}$ , attributed to the N–H, C–H, C=O and C=C stretching vibrational modes, respectively, confirming the presence of the biotemplate in the hybrid material. After heat treatment at 700 °C for 3 h, those peaks disappeared (Figure 5c) indicating the decomposition of the biotemplate and formation of ZnO. The strong absorption band at 500  $\text{cm}^{-1}$  is characteristic of ZnO nanostructure vibrations.<sup>31</sup> A broad band appearing at 3422  $\text{cm}^{-1}$  is related either to water or hydroxyl groups adsorbed on the ZnO surface, as confirmed by the peaks in the 1100 to 1650  $\text{cm}^{-1}$  range, that can be assigned to the bending modes of hydroxyl groups.<sup>3</sup>

#### Photoluminescence study

The room temperature photoluminescence (PL) spectrum of brush-like ZnO nanorods is consistent with that previously

reported in the literature,<sup>32,33</sup> as shown in Figure 6. The broad emission band centered at 425 nm can be attributed to the radiative recombination of electrons in the conduction band with holes in the valence band, while the strong and narrow blue emission at 480 nm probably is originated from the recombination of oxygen vacancies or other defects with interstitial oxygen. The green emission peak centered at 535 nm is attributed to the recombination of singly ionized oxygen vacancy with photogenerated holes.<sup>34-38</sup> The UV absorption spectrum of a dispersion of ZnO nanorods in ethanol, exhibiting a broad absorption band at 374 nm, is shown in the inset of Figure 6. That band is not found in the bulk material. The PL spectrum was blue shifted and consistent with a band gap of  $E_g = 3.51$  eV, in comparison with bulk ZnO (3.47 eV). In fact, the band gap depends on the particle size and morphology of nanoparticles, as reported by Yadav *et al.*<sup>39</sup> Vanheusden *et al.*,<sup>40</sup> who proposed that the green emission can be assigned to the recombination of photogenerated holes with electrons occupying singly ionized oxygen vacancies. Huang *et al.*,<sup>41</sup> suggested that there is a relatively large concentration of oxygen vacancies in the nanowires because a progressive increase of the green light emission intensity was observed, relative to the UV emission, as the nanorods diameter decreased.

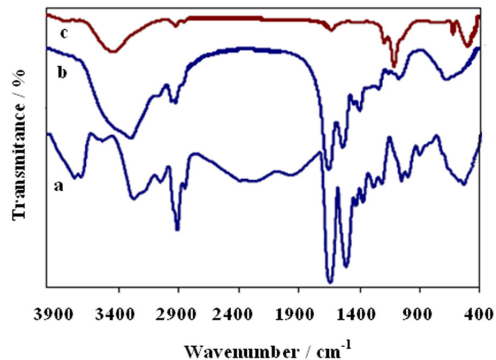


**Figure 5.** FTIR spectra of (a) albumen, (b) as-prepared Zn(II)/albumen hybrid, (c) brush-like ZnO nanorods obtained after calcination at 700 °C, for 3 h.

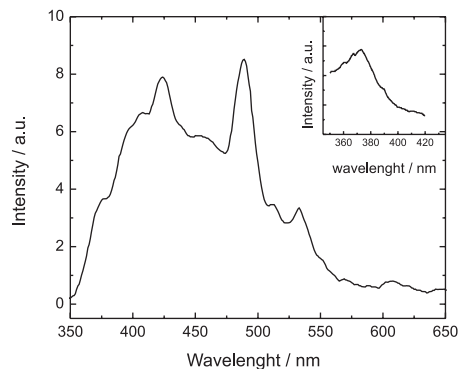


**Figure 6.** Absorption (inset) and PL spectrum of ZnO nanorods ( $\lambda_{\text{exc}} = 230$  nm).

## Conclusions

Brush-like ZnO nanorods were successfully prepared by one-pot reaction of Zn(II) acetate with albumen as biotemplate in water, by the sol-gel method, and subsequent heat treatment of the hybrid at 700 °C. The biotemplate was completely removed after calcination leading to the formation of highly crystalline brush-like ZnO nanorods with wurtzite-like structure. The material has a narrow size distribution and average diameter of about 90 nm and  $\geq 1$   $\mu\text{m}$  length. The surface area was found to be 6.91  $\text{m}^2 \text{g}^{-1}$ . Particularly significant is the role of the biotemplate that induced the formation of nanorods with specific morphology of nano-brushes. Surface defects are expected based on the PL spectra and SAED of the nanomaterial, which should be suitable for application in photocatalytic reactions.

## Acknowledgments

This work was financially supported by the University of Alzahra.

## References

1. Fernandez-Garcia, M.; Martinez-Arias, A.; Hanson, J. C.; Rodriguez, J. A.; *Chem. Rev.* **2004**, *104*, 4063.
2. Takahashi, N.; *Mater. Lett.* **2008**, *62*, 1652.
3. Li, Q.; Kumar, V.; Li, Y.; Zhang, H.; Marks, T. J., Chang, R. P. H.; *Chem. Mater.* **2005**, *17*, 1001.
4. Zhang, J.; Sun, L.; Pan, H.; Liao, C.; Yan, C.; *New J. Chem.* **2002**, *26*, 33.
5. Li, M.-K.; Wang, D.-Z.; Ding, Y.-W.; Guo, X.-Y., Ding, S.; Jin, H.; *Mater. Sci. Eng., A* **2007**, *452-453*, 417.
6. Fang, F.; Zhao, D. X.; Zhang, J. Y.; Shen, D. Z.; Lu, Y. M.; Fan, X. W.; Li, B. H.; Wang, X. H.; *Mater. Lett.* **2008**, *62*, 1092.
7. Zhang, Q.; Zhang, Y.; Yu, K.; Zhu, Z.; *Vacuum* **2008**, *82*, 30.
8. Zhang, B. P.; Binh, N. T.; Wakatsuki, K.; Segama, Y.; Yamada, Y.; Usami, N.; Kawasaki, M.; Koinuma, H.; *Appl. Phys. Lett.* **2004**, *84*, 4098.
9. Yu, H.; Zhang, Z.; Han, M.; Hao, X.; Zhu, F.; *J. Am. Chem. Soc.* **2005**, *127*, 2378.
10. Jia, Z.; Yue, L.; Zhang, Y.; Xu, Z.; *Mater. Chem. Phys.* **2008**, *107*, 137.
11. Zhang, J.; Yu, W.; Zhang, L.; *Phys. Lett. A* **2002**, *299*, 276.
12. Umar, A.; Hahn, Y. B.; *Nanotechnology* **2006**, *17*, 2174.
13. Lao, J. Y.; Huang, J. Y.; Wang, D. Z.; Ren, Z. F.; Steeves, D.; Kimban, B.; Porter, W.; *Appl. Phys. A: Mater. Sci. Process.* **2004**, *78*, 539.
14. Du, G. H.; Xu, F.; Yuan, Z. Y.; Van Tendeloo, G.; *Appl. Phys. Lett.* **2006**, *88*, 243101.

15. Fang, Z.; Tang, B. K.; Shen, G.; Chen, D.; Kong, R.; Lei, S. J.; *Mater. Lett.* **2006**, *60*, 2530.
16. Wang, J.; Cao, J.; Fang, B.; Lu, P.; Deng, S.; Wang, H.; *Mater. Lett.* **2005**, *59*, 1405.
17. Li, C.; Fang, G.; Guan, W.; Zhao, X.; *Mater. Lett.* **2007**, *61*, 3310.
18. Yang, Y.; Chen, H.; Zhao, B.; Bao, X.; *J. Cryst. Growth* **2004**, *263*, 447.
19. Saravandan, P.; Alam, S.; Mathur, G. N.; *Mater. Lett.* **2004**, *58*, 3528.
20. Tonto, P.; Mekasuwandumrong, O.; Phatanasri, S.; Pavarajan, V.; Praserttham, P.; *Ceram. Int.* **2008**, *34*, 57.
21. Gu, X.; Nie, C.; Lai, Y.; Lin, C.; *Mater. Chem. Phys.* **2006**, *96*, 217.
22. Zhang, H.; Yang, D.; Li, S.; Ma, X.; Ji, Y.; Xu, J.; Que, D.; *Mater. Lett.* **2005**, *59*, 169.
23. Ye, Z. Z.; Yang, F.; Lu, Y. F.; Zhi, M. J.; Tang, H. P.; Zhu, L. P.; *Solid State Commun.* **2007**, *142*, 425.
24. Liu, B.; Zeng, H. C.; *J. Am. Chem. Soc.* **2003**, *125*, 4430.
25. Mandelaers, D.; Vanhoyland, G.; Van den Rul, H.; Hean, J. D.; VanBeal, M. K.; Mullens, J.; Van Poucke, L. C.; *Mater. Res. Bull.* **2002**, *37*, 901.
26. Uekawa, N.; Iahii, S.; Kojima, T.; Kakegawa, K.; *Mater. Lett.* **2007**, *61*, 1729.
27. Li, M.; Bala, H.; Lu, X.; Ma, X.; Sun, F.; Tang, L.; Wang, Z.; *Mater. Lett.* **2007**, *61*, 690.
28. Bauermann, L. P.; Bill, J.; Aldinger, F.; *J. Phys. Chem. B* **2006**, *110*, 5182.
29. Dai, Y.; Zhang, Y.; Bai, Y. Q.; Wang, Z. L.; *Chem. Phys. Lett.* **2003**, *37*, 596.
30. Bhattacharyya, S.; Gdanken, A.; *Microporous Mesoporous Mater.* **2008**, *110*, 553.
31. Li, J.; Zhao, X.; Yan, C.; Yijing, L.; *Mater. Chem. Phys.* **2008**, *107*, 177.
32. Lupan, O.; Chow, L.; Chai, G.; Roldan, B.; Naitabdi, A.; Schulte, A.; Heinrich, H.; *Mater. Sci. Eng., B* **2007**, *145*, 57.
33. Uthirakumar, P.; Karunakaran, B.; Nagarajan, S.; Suh, E.-K.; Hong, C.-H.; *J. Cryst. Growth* **2007**, *304*, 150.
34. Kale, R. B.; Hsu, Y. J.; Lin, Y. F.; Lu, S. Y.; *Solid State Commun.* **2007**, *142*, 302.
35. Khan, A.; Jadwisieniczak, W. M.; Lozykowski, H. J.; Kordesch, M. E.; *Physica E* **2007**, *39*, 258.
36. Fang, F.; Zhao, D. X.; Zhang, J. Y.; Shen, D. Z.; Lu, Y. M.; Fan, X. W.; Li, B. H.; Wang, X. H.; *Mater. Lett.* **2008**, *62*, 1092.
37. Chen, B. J.; Sun, X. W.; Xu, C. X.; Tay, B. K.; *Physica E* **2004**, *21*, 103.
38. Zhai, H. J.; Wu, W. H.; Lu, F.; Wang, H. S.; Wang, C.; *Mater. Chem. Phys.* **2008**, *112*, 1024.
39. Yadav, R. S.; Mishra, P.; Pandey, A. C.; *Ultrasound. Sonochem.* **2008**, *15*, 863.
40. Vanheusden, K.; Warren, W. L.; Seager, C. H.; Tallant, D. R.; Voigt, J. A.; Gnade, B. E.; *J. Appl. Phys.* **1996**, *79*, 7983.
41. Huang, M. H.; Wu, Y. Y.; Feick, H. N.; Ttran, N.; Weber, E.; Yang, P. D.; *Adv. Mater.* **2001**, *13*, 113.

Submitted: March 30, 2010

Published online: October 26, 2010